ICANS-XIV
14th Meeting of the International Collaboration on
Advanced Neutron Sources
June 14-19,1998
Starved Rock Lodge Utica,IIIinois,USA

Analyses on Pressure Wave Propagation and Dynamic Stress in Mercury Targets

Syuiti Ishikura, Masanori Kaminaga, Akira Susuki, Ryutaro Hino
Japan Atomic Energy Research Institute,JAPAN
Iwao Harada, Kosuke Kamba and Motoaki Sakashita
Hitachi Ltd.,JAPAN

ABSTRACT

Stress and pressure are analyzed for solving the main design problem in the JAERI 5MW liquid mercury target. Two different codes are used to evaluate the stress and pressure waves under a single pulsed heating. They are the structural analysis code and a developed liquid mercury program. Stress waves are computed in an axisymmetric target container coupled with liquid approximated as solid with compressibility. Pressure waves are computed in the target liquid treated as a purely liquid mercury extending TVD(Total Variational Diminishing) in gas to liquid.

The maximum stress 170MPa appears as the meridional stress at the window center, because the bending stress increases for a rectangular beam profile. As beam profiles change from rectangular to parabola, the meridional stress decreases at the value of 100MPa which is smaller than the circumferential stress value 110-130MPa.

The developed program well shows generation, propagation and reflection of the pressure wave. Pressures become 100MPa at the window center and 60 MPa at the cylinder surface.

1 Introduction

A major design problem in neutron spallation source is how to design the structure of the target in consisting with complicated dynamic load generated by pressure waves. A liquid mercury target has been expected as a next generation liquid metal target to produce much more neutrons than a solid target. They are

planning as SNS(Spallation Neutron Source), ESS(European Spallation Source) and NSF(Neutron Spallation Facility) of JAERI using the 5MW liquid mercury target.

From a view point of physical understanding, elastic or stress waves generated in solid have been well known by Love's famous study [1] . Also, stress waves can be computed by the structural analysis code such as ANSYS or ABAQUS. A solid target can be designed within structural dynamics.

A few means exist to know the pressure wave mechanism generated in liquid, because liquid state is not clarified comparing with solid and gas. Skala and Bauer[2] computed the pressure wave using the extension from the structural analysis. The PSI developed KASKA program[3] based on the Lagrange/Finite Difference Method. However, the equation of state is not given such as an equation of perfect gas so that the lack of the equation of state causes a difficulty of liquid metal target design. Solving this difficulty, the liquid program based on TVD (Total Variational Diminishing) have been developed reconstructing TVD theory in gas dynamics to apply the liquid mercury target.

In this report, stress and pressure are independently analyzed for the JAERI 5MW liquid mercury target under a single pulsed heating by using ABAQUS-Explicit code and the developed program. Stress waves are computed in an axisymmetric target container coupled with liquid approximated as a solid with compressibility. Pressure wave is computed in detail as the process of generation, propagation and reflection of the compression and rarefaction waves.

2 Analysis models of 5MW mercury targets

Fig.1 shows analysis models of the JAERI 5MW liquid mercury target used for computations. A basic profile is a rectangular flat beam of 93.6mm diameter. Profiles are changed other parabolic, Gaussian distributions in the radial direction as a computational parameter. The energy deposition varies with both axial and radial positions. The axial beam profile is expressed by an approximate function obtained from Monte Carlo code NMTC/JAERI[4]. The energy deposition per one pulse is shown in fig.1 as a time average of 50Hz. The target is composed with a dome-shaped window and a cylinder of 200mm diameter, 1100mm length and 2.5mm thick. Liquid mercury is kept at 52°C until the first pulse arriving. After the pulse, the temperature difference reaches the maximum 19.5°C at the axial distance 15mm from the window center.

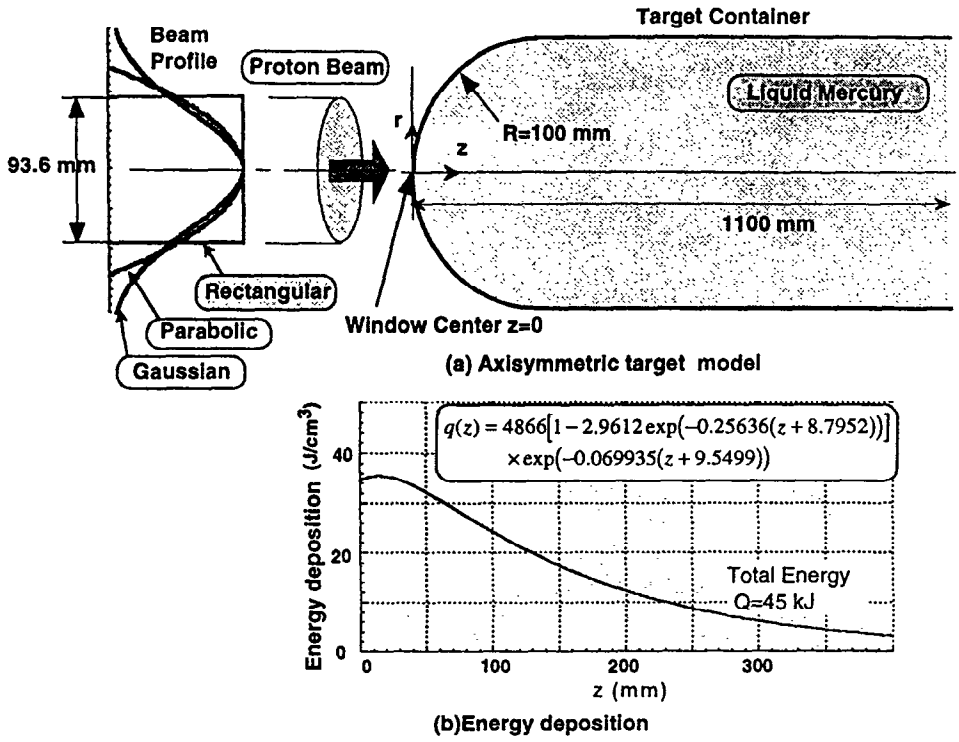

Fig.1 Stress wave analysis model of 5MW mercury targets

3 Structural analysis

3.1 Computational parameters

An axisymmetric co-ordinate system r and z is used through both analyses, where r and z are coordinates in the radial and axial direction, respectively. The window center locates at $z = 0$. Computations are made on the shell container coupled with liquid mercury by using ABAQUS-Explicit FEM code. Liquid mercury is modeled as an incompressible solid, where modulus of elasticity 6.6MPa is small enough and the Poisson's ratio 0.49995 is close to 0.5. Numbers of elements are 235 and 11125 in the container and liquid mercury, respectively. The size of elements is 2mm in the radial direction, and is from 2mm to 10mm in the axial direction.

3.2 Stress on a target container

Fig.2 shows a schematic diagram of the generation and propagation of the stress and pressure waves at early time. In a liquid target, two pressure wave fronts are generated at an interface between cold and heated liquids due to thermal expansion of liquid. One is formed at the intersection between window and cylinder

of beam diameter near the window center. The other is the liquid surface of the cylinder which has the same beam diameter. The first wave continuously acts on the window wall in the axial direction from an initial time. The second wave reaches lately to the cylinder surface of the container traveling the cold liquid in the radial direction. Fig.3 shows the time history of the meridional stress at various

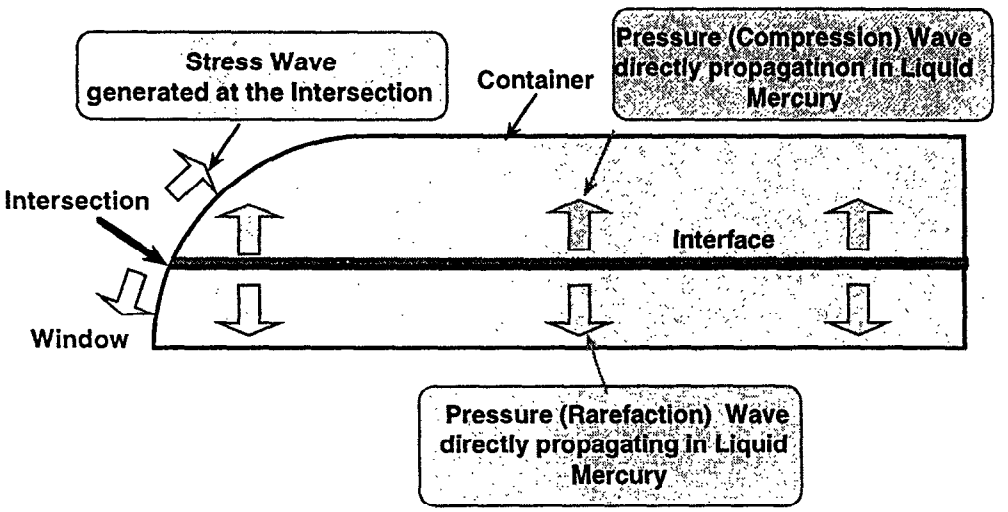

Fig.2 A schematic diagram of generation and propagation of stress and pressure waves

axial positions of the container. It seems that stress at the window center z=0mm behaves differently from these at other positions z=10-50cm in the cylinder. The essential difference is caused by other reason where the tip location is a singular point of the doom-shape container. Fig.4 shows the time history of the meridional stress at the window center. It is easily understood that the bending moment is added to the membrane force. As shown in fig.3, the same stress wave travels from forward (the intersection) to backward (z=10-50cm). The delayed time agrees with a propagation time 20 μ s in which the elastic wave travels the distance 10cm at sound velocity 4890m/s. Then, the meridional stress attains the maximum value 170MPa at the window center z=0mm.

Fig.5 shows the time history of the circumferential stress at various axial positions of the container. It is seen that stress at the positions z=10cm increases firstly and after the time, the stress at other positions z=20-50cm changes simultaneously. The time difference corresponds to the difference of sound velocities of solid and liquid. It takes 20 μ s the stress wave in solid arriving at z=10cm,but the pressure wave in liquid can arrive at the same position in 45 μ s. Then, the the circumferential stress at z=10cm is produced by the stress wave traveling from the

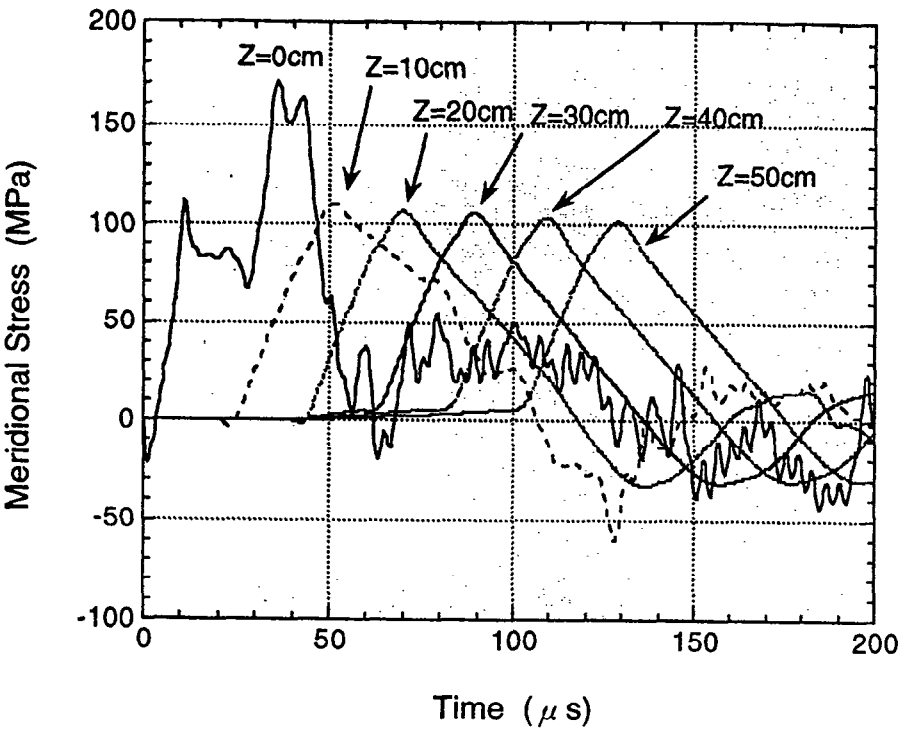

Fig.3 Meridional stress in the target container

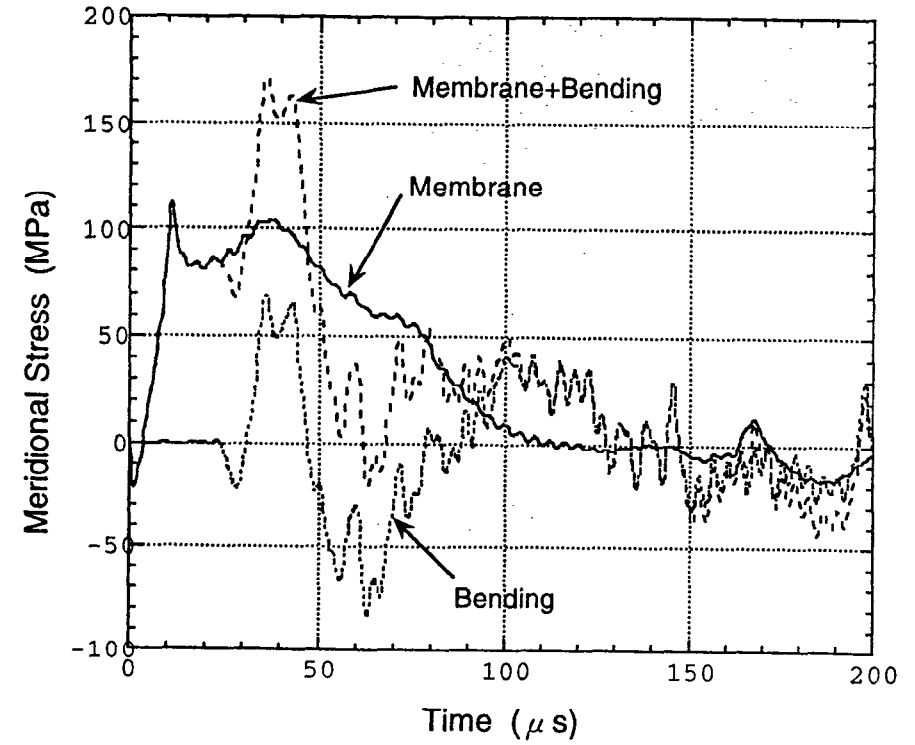

Fig.4 Meridional stress at the window center

intersection. The stress at z=20-50cm is directly produced by the pressure wave traveling from the cylindrical liquid surface of the beam diameter. The stress appears as the maximum stress 130MPa for the different wave pass. The energy deposit affects the strength and profiles of stress which decrease to backward.

Next, the beam profiles are changed expecting the reduction of meridional

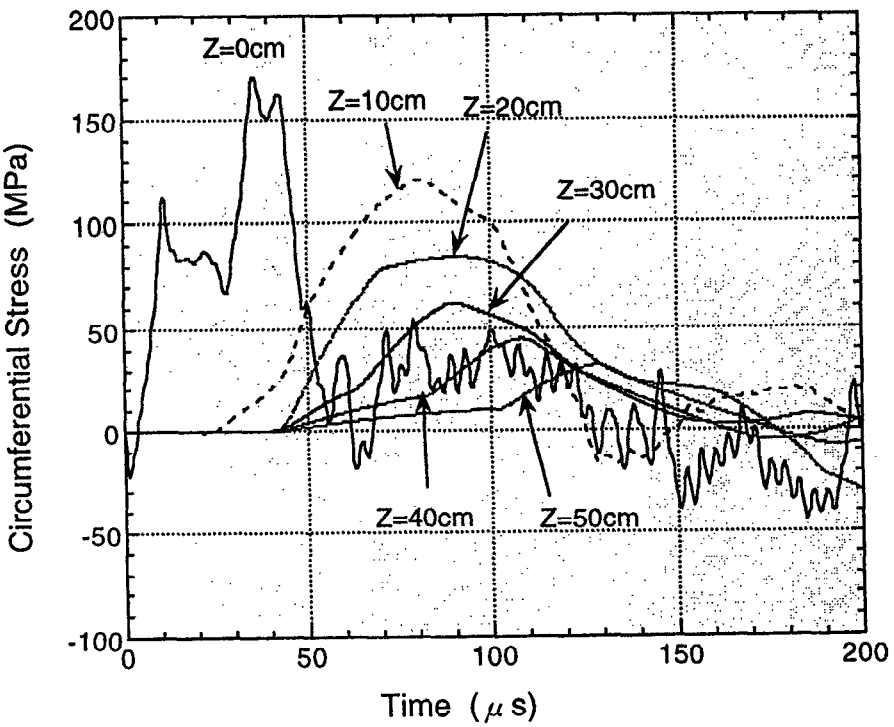

Fig.5 Circumferential stress in the target container

stress,especially, bending moment at the wind center. These profiles are parabolic and Gaussian distributions. Fig.6 shows the effects of beam profiles on meridional stress. It can be seen that the maximum stress 100MPa for both beam profiles is much smaller than the value 170MPa for the rectangular beam profile. This is because the force of the pressure wave decreases at the interface due to the small temperature gradient between cold and heated liquids.

4 Liquid target analysis

4.1 Numerical method and parameters

An axisymmetric compressible Euler equation are employed as the governing equations. The TVD scheme with Roe's flux difference splitting [5] is

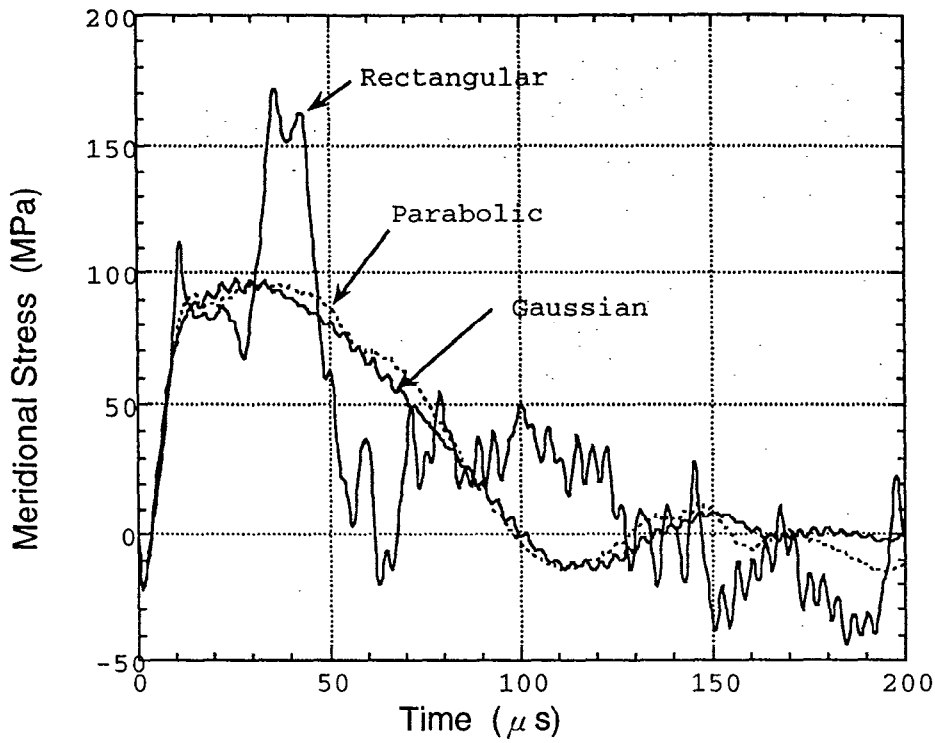

Fig.6 Beam profile effects on meridional stress at the window center

reconstructed for the state equation of liquid (which is the Tait equation, not the Mie-Grüneisen equation), because the original Roe's scheme is derived from the state equation of a perfect gas. The liquid target program is developed on the basis of TVD/Finite Volume Method.

Fig.7 shows the pressure wave analysis model of the JAERI 5MW liquid mercury target. The rectangular beam case is only computed in detail to investigate the generation and propagation process of the pressure waves in the liquid mercury. It is assumed that the wave fully reflects on the wall. The slip condition is adopted on the wall. Fig.8 shows a grid system used for pressure wave computation. The computational region is divided into 600 × 100 cells in the radial and axial directions, respectively. The cell size is about 1 mm square near the target window as shown in fig.8.

4.2 Pressure wave propagation in targets

Fig.9 shows the time history of the pressure in the liquid mercury of the wall. The tracer points are located at z =0 mm, 30 mm, and 100 mm, where z is a coordinate in axial direction and $z = 0$ representsat the center of the target window. In fig.9 the time **a**~**m** correspond to the peaks of the pressure history curves. In the following paragraphs, we will describe the propagation process of

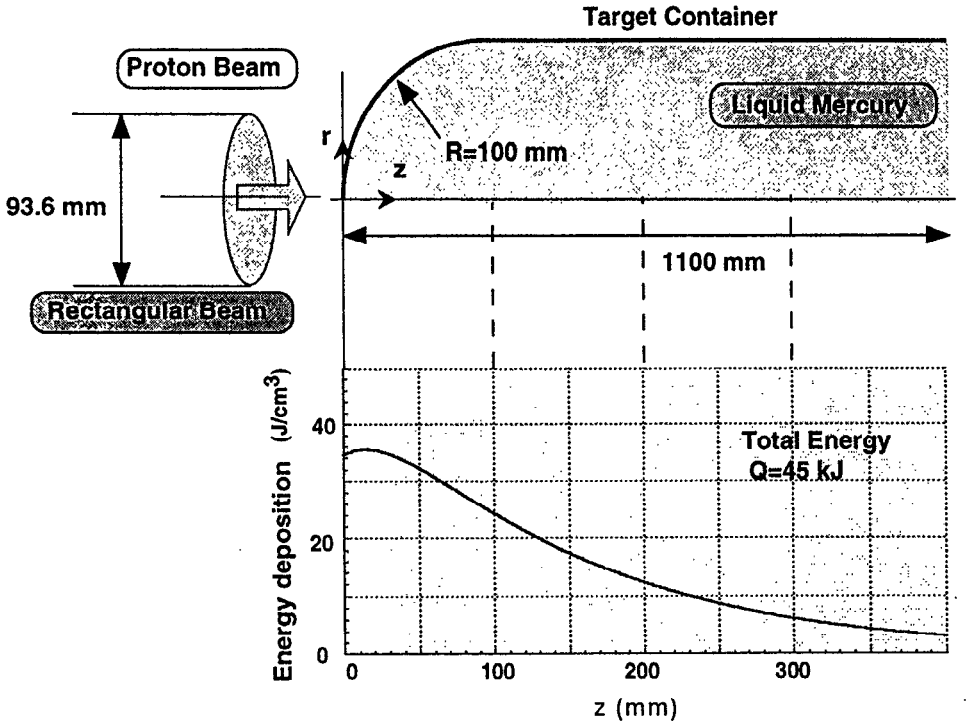

Fig.7 Pressure wave analysis model of 5MW mercury targets

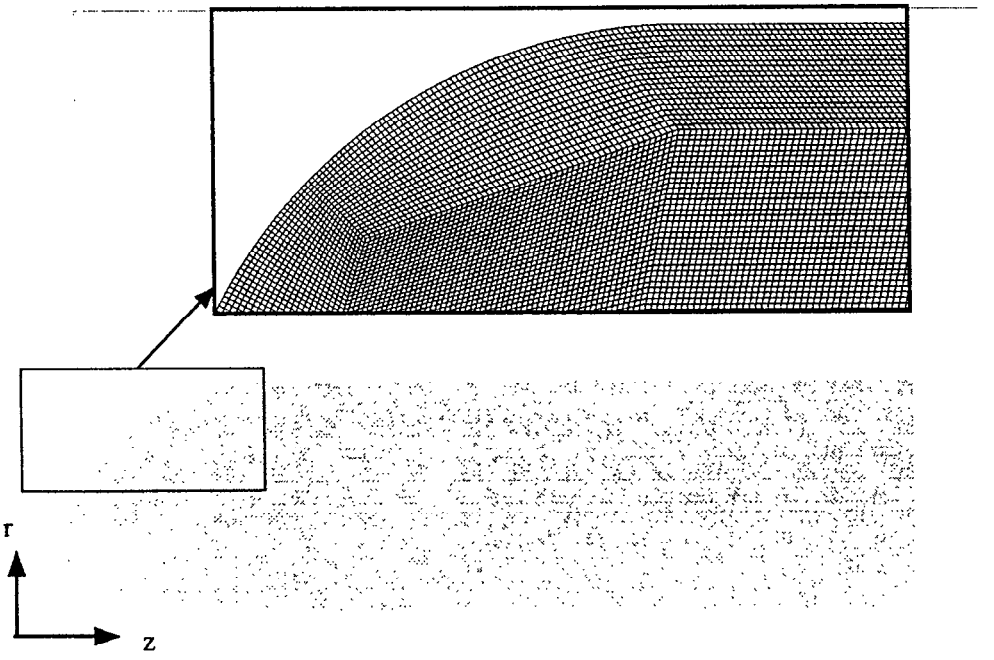

Fig.8 A grid system used for pressure wave computations (100 X600 cells)

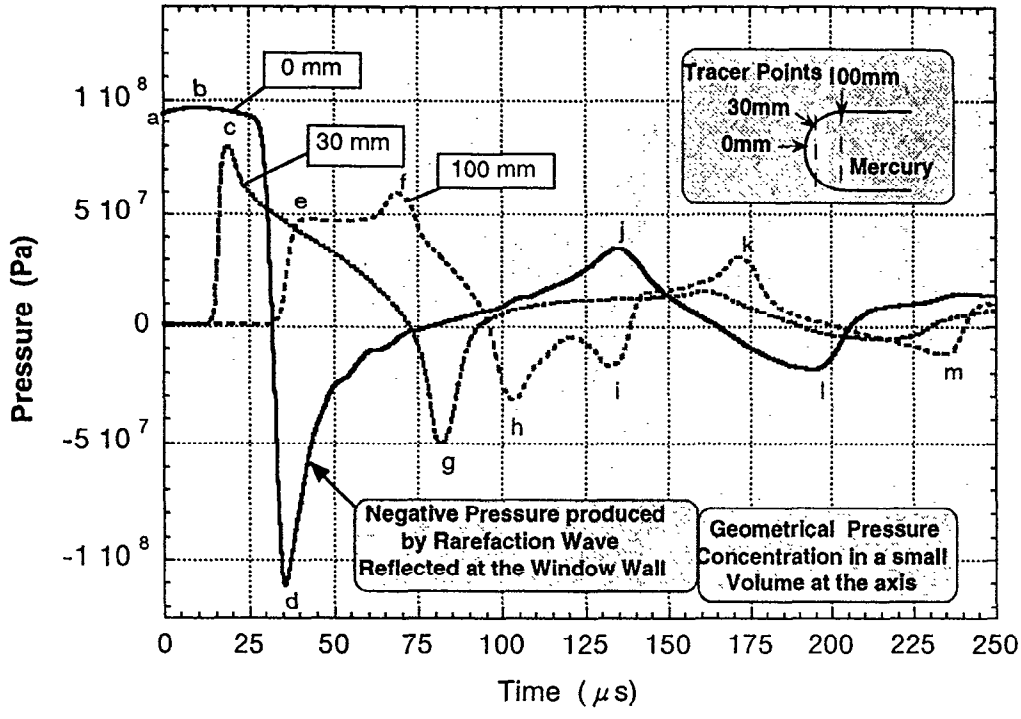

Fig.9 Time history of pressure waves on the mercury surface

pressure waves at each time **a**~**m**. For the help of the comprehension, fig.10 shows the pressure wave propagation in the mercury target represented by the pressure contours at the time **a** ($t = 0$ μs), the time **c** ($t = 26$ μs), the time **f** ($t = 50$ μs) and after. Fig.11 gives the schematic diagram of pressure wave propagation at the time **f**.

To begin with, we will classify pressure waves in a usual way. When a proton beam is pulsed, two types of pressure waves— compression wave and rarefaction wave — generate at the same time. From the path waves have traveled along, another category — direct wave and reflected wave —comes, namely,a direct wave is the wave that has come directly from the point of generation whereas a reflected wave is the wave that has come after it has reflected by walls. Pressure waves are classified with the combination of these two categories. For example, a direct compression wave is defined by the condition that it is a compression wave and it has come directly from the point of generation. The classification may be unworkable if those waves have reflected many times, but at the initial stage, it is very useful to describe the propagation process of waves. At the time **a** (the initial condition), the deposited heat determines the pressure distribution, and the pressure at the point 0 mm becomes high. The highest pressure is, then, observed at z =15 mm. Assuming the sound speed to be equal to 1450 m/s in the liquid mercury, it takes 0.015(m)/1450(m/s) = 10 μs for the highest pressure 95MPa to

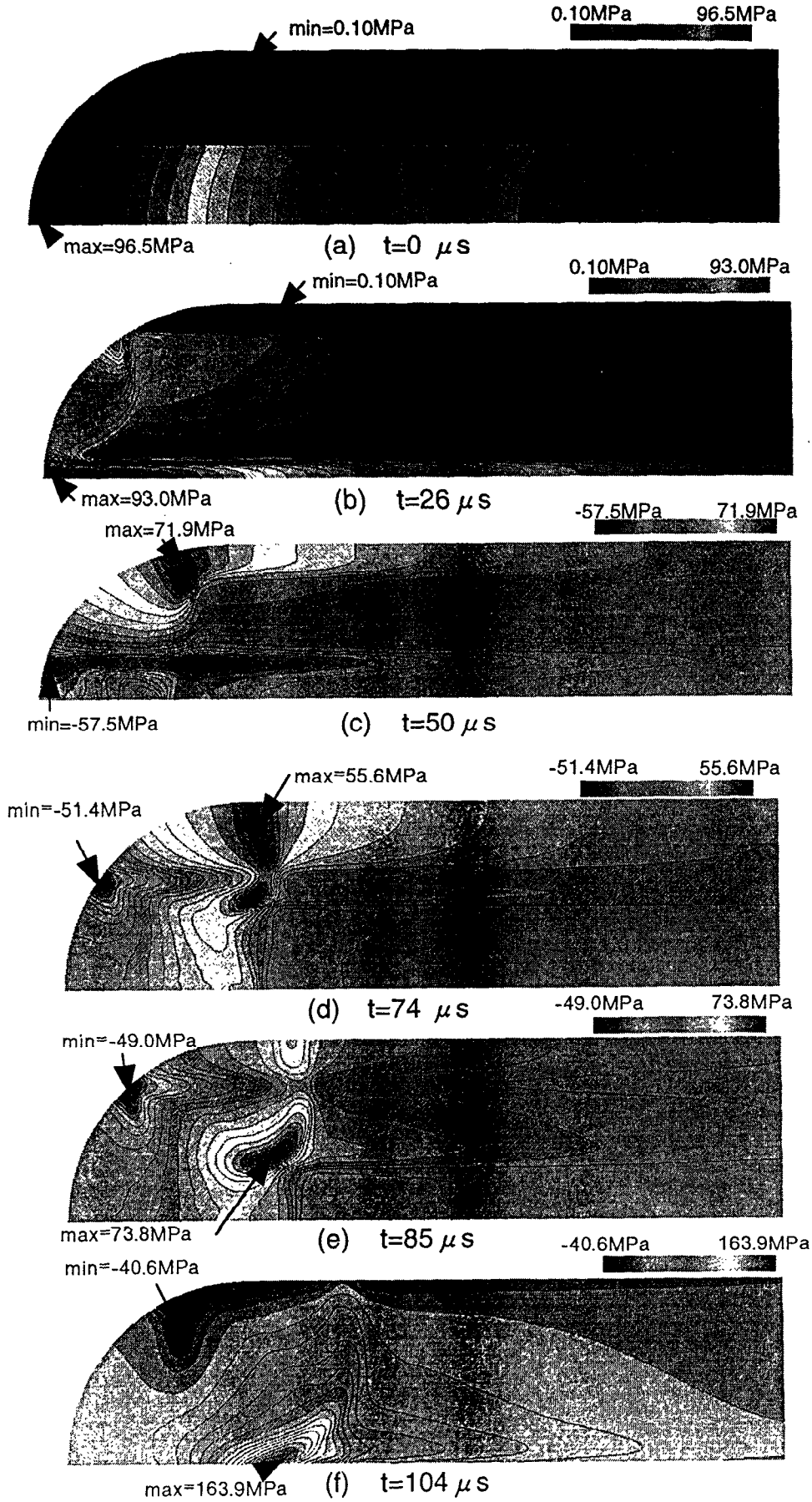

Fig.10 Pressure wave propagation in the mercury target

travel to the target window (z =0 mm). The time 10 μs agrees with the peak time **b** (13 μs) in fig.9.

At the time **c**, the pressure at the point 30 mm increases because two compression waves — the direct compression wave which has come directly and the reflected compression wave which has reflected by the target window wall— reach the point 30 mm at the same time. The pressure at the point 100 mm changes in a different way, because the direct compression wave reaches there ahead of the reflected compression wave at the time **e**, whereas the reflected compression wave reaches the point of the pressure 60MPa at the time **f**. The different time **e** and **f** correspond to the different distance which each wave has traveled. The direct compression wave has traveled the distance between the beam radius 46.8 mm and the target cylinder radius 100 mm, and it reaches the point 100 mm at $(0.1 - 0.0468)(\mathrm{m})/1450(\mathrm{m/s}) = 37$ μs, which agrees with the time **e** (39 μs). On the other hand, the reflected compression wave has traveled 109 mm which is measured along the target wall, and it reaches the point 100 mm at $0.109(\mathrm{mm})/1450(\mathrm{m/s}) = 75$ μs,which agrees with the time **f** (74 μs).

The direct compression wave travels across the target cylinder before it reaches again the point 100 mm after the time **e**. It takes $0.2(\mathrm{m})/1450(\mathrm{m/s}) = 140$ μs, then it reach the point at t =180 μs, which agrees with the time **k**. The rarefaction

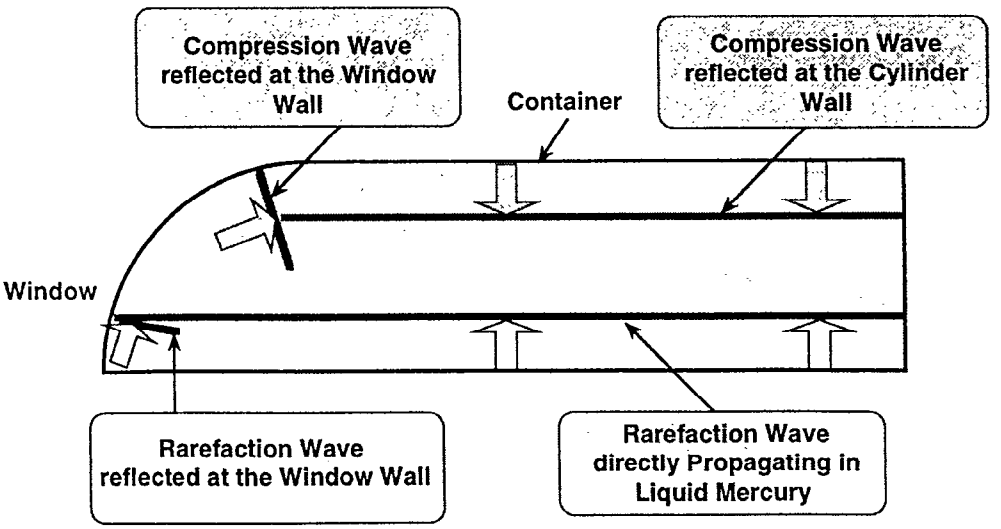

Fig.11 A schematic diagram of pressure wave propagation at t=50 μ s

waves propagate similarly. At the time **d**, the liquid mercury on the axis suffers severe negative pressure because the rarefaction wave are focused there (although such severe negative pressure does not occur in the real liquid mercury). At the

time **g**, the pressure at the point 30 mm become negative because two rarefaction waves — the direct rarefaction wave which has come directly and the reflected rarefaction wave which has reflected by the target window wall—reach there at the same time. The direct rarefaction wave reaches the point 100 mm ahead of the reflected rarefaction waves at the time **h**, and the reflected rarefaction wave reaches the point at the time **i**. Like the case of compression waves, the different time **h** and **i** correspond to the different distance each wave has traveled, though the difference 31 μs is shorter than the difference 37 μs observed in the case of compression waves.

The direct rarefaction wave reaches the point 100 mm at 140 μs after the time **h**, i.e., at t =250 μs, which agrees with the peak at the time **m**.

In the later stage, compression waves and rarefaction waves discussed above go on propagating. The time histories of the pressure become complicated because more reflected waves are generated at the target window and they interfere each other,but they still oscillate in the same cycle 140 μs.

5 Summary

Stress and pressure are analyzed for solving the main design problem in the JAERI 5MW liquid mercury target. Two different codes are used to evaluate the stress and pressure waves under a single pulsed heating. They are the structural analysis ABAQUS-Explicit code and a developed liquid mercury program. Stress waves are computed in an axisymmetric target container coupled with liquid approximated as a solid with compressibility. Pressure waves are computed in target liquid treated as a purely liquid mercury extending TVD(Total Variational Diminishing) in gas to liquid.

The maximum stress 170MPa appears as the meridional stress at the wind center, because the bending stress increases for a rectangular beam profile. As beam profiles change from rectangular to parabola, bending stress decreases at the tip. Then meridional stress decreases at the value of 100MPa which is smaller than the circumferential stress value 110-130MPa.

The developed program well shows generation, propagation and reflection of the compression and rarefaction waves. Pressures become 100MPa at the window center and 60 MPa at the cylinder surface.

In the present analyses, the stress is not so high, but this is the first step to evaluate the dynamic stress generated in liquid metal target. The next steps have to be considered are to predict accurate stress values. First, it is necessary to combine liquid and structure analyses for comparing numerical results with exper-

iments. Secondly, the target is approximated as an axisymmetric container that is a suitable geometry to experiments. The practical shape is between two and three dimensional, so that three dimensional analysis is required to make practical design.

References

[1] A.E.H. Love, "A Treatise on the Mathematical Theory of Elasticity" Dover Publications, New York,(1963)

[2] K.Skala and G.S.Bauer, "On the pressure wave problem in liquid metal targets for pulsed spallation neutron sources ", ICANS-XIII, Vol.2, Switzerland, (1995)

[3] L.Ni, (private communication)

[4] H.Takada, N.Yoshizawa, K.Kosaka and K.Ishibashi, "An Upgrade Version of the Nucleon Transport Code:NMTC/JAERI97", JAERI-Data/Code, 98-005 in Japanese, (1998)

[5] P.L.Roe, "Approximate Riemann Solvers, Parameter Vectors, and Difference Schemes", *Journal of Computational Physics* **43**, p.357-372, (1981)